Determination of the ^{8}B Neutrino Spectrum

W. T. Winter and S. J. Freedman
Nuclear Science Division, Lawrence Berkeley National Laboratory, Berkeley, California 94720, USA
Physics Department, University of California, Berkeley, California 94720, USA

K. E. Rehm, I. Ahmad, J. P. Greene, A. Heinz, D. Henderson, R. V. F. Janssens, C. L. Jiang, E. F. Moore, G. Mukherjee, R. C. Pardo, T. Pennington, G. Savard, J. P. Schiffer, D. Seweryniak, and G. Zinkann
Physics Division, Argonne National Laboratory, Argonne, Illinois 60439, USA

M. Paul
Racah Institute of Physics, Hebrew University, Jerusalem, Israel 91904
(Received 19 March 2003; revised manuscript received 22 September 2003; published 18 December 2003)

We have measured the total energy of the alpha particles following the beta decay of ^{8}B by implanting ^{8}B into a planar silicon surface barrier detector. Calibration was performed using alpha particles following the beta decay of ^{20}Na, similarly implanted. The alpha spectrum is used to infer the ^{8}B neutrino spectrum which is an important input in the interpretation of experiments that detect energetic neutrinos from the Sun. The alpha spectrum reported here is in disagreement with the previous best measurement which used two detectors in coincidence.

DOI: 10.1103/PhysRevLett.91.252501 PACS numbers: 23.40.Bw, 23.60.+e, 26.65.+t, 27.20.+n

The solar neutrino problem originated in 1968 when the novel Homestake ^{37}Cl capture experiment [1] placed a limit on the solar neutrino flux that was less than half of solar model predictions [2]. Additional solar neutrino data have since been collected by the Gallex, SAGE, and GNO ^{71}Ga capture experiments and the Kamiokande, Super-Kamiokande, and Sudbury Neutrino Observatory (SNO) water Cherenkov experiments [3]. Flux measurements from different reactions are inconsistent with each other and with current solar model predictions [4] when standard electroweak theory is assumed. Matter-enhanced flavor oscillations due to finite neutrino mass offer a resolution of the discrepancy. Recent measurements of charged- and neutral-current ν-d scattering at SNO provide direct evidence that solar neutrinos are indeed changing flavor [5]. Global analyses of solar neutrino data [3] show that neutrino oscillation scenarios yield adequate agreement between experiments and solar models. Recent evidence from the KamLAND reactor antineutrino experiment supports the oscillation interpretation [6].

Neutrinos from the β decay of ^{8}B, produced in the solar core, account for a majority of the ^{37}Cl capture events, and Super-Kamiokande and SNO are sensitive to the differential ^{8}B neutrino spectrum. A determination of the physics of leptonic flavor mixing from observations of the solar neutrino spectral shape requires an understanding of the decay of ^{8}B, shown in Fig. 1. The neutrino spectrum of an allowed β decay between two *sharp* nuclear states is well understood; in the case of ^{8}B, the neutrino spectrum depends strongly on the excitation energy profile of the α-unstable ^{8}Be daughter, which must be determined experimentally.

The resonance structure of ^{8}Be has been investigated by α-α scattering [7,8], and β-delayed α-spectrum measurements in both ^{8}B and ^{8}Li [9–12]. The R-matrix formalism has been used to extract nuclear level parameters and to attempt to relate the various processes [13–16]. Such a comparison is subject to corrections that may be significant. The transition matrix elements in the β decay depend on the radial wave functions of the ^{8}B(^{8}Li) ground state and the ^{8}Be continuum, and are thus dependent on ^{8}Be excitation energy. The R-matrix approach does not correctly include this dependence, a deficiency which may lead to disagreement between the nuclear parameters extracted from various processes. A direct determination of the ^{8}B neutrino spectrum, independent of the R-matrix formalism, is provided by measurement of the ^{8}B β-delayed α spectrum.

Previous measurements of the α spectrum involved the production of ^{8}B ($t_{1/2} = 778$ ms) which was stopped in a catcher foil and then positioned adjacent to a Si detector.

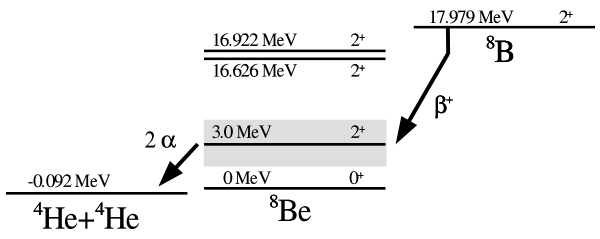

FIG. 1. Nuclear levels relevant to the ^{8}B decay chain (not to scale). The β decay proceeds through the broad 2^+ resonance structure in ^{8}Be peaked at an excitation energy of 3.0 MeV with a width of 1.5 MeV. Decay to the 0^+ ground state in ^{8}Be is second forbidden and is highly suppressed.

Energy deposition in the detector was measured and corrections were made for energy losses in the catcher foil and detector dead layer. The first four experiments, by Farmer and Class [9], Wilkinson and Alburger with both a thick and thin catcher foil [11], and De Braeckeleer and Wright [10], observed the singles α spectrum. Data from these four measurements differ from each other by energy offsets of order 100 keV, an effect attributed to systematic problems with detector calibration and energy loss in the dead layer [17].

The β spectrum of ^{8}B, like the neutrino spectrum, depends on the excitation energy profile of the broad ^{8}Be resonance. A precise measurement of the β spectrum above 9 MeV has been performed using a 180° magnetic spectrograph [18]. The singles α-spectrum data and β-spectrum data have been used to predict a neutrino spectrum, based on varying assumptions [17–19].

Recently, the coincidence α spectrum was measured by Ortiz *et al.* using two detectors [12]. A 3.5 T magnetic field produced by a superconducting solenoid channeled the β particles away from the detectors, eliminating a systematic effect shared by previous measurements. The field also affected the α trajectories and a simulation based on ^{4}He charge state fractionation was necessary to adjust the data. Both the SNO and Super-Kamiokande collaborations [5,20] interpreted their data using the ^{8}B neutrino spectrum recommended by Ortiz *et al.*

The experiment described here was designed to minimize systematic effects present in the previous α-spectrum measurements. A beam of ^{8}B ions was implanted near the midplane of a planar Si detector, which eliminated α-particle energy loss in insensitive regions and allowed the sum energy of the two α particles to be observed with a single detector. The energy deposited by β particles was minimized by the use of a thin (91 μm) Si detector, just sufficient to stop the most energetic α particles, and by the requirement of a coincidence count in a plastic scintillation β detector which defined the trajectories of the β particles. For calibration, ^{20}Na ions were implanted into the same detector immediately before the ^{8}B measurement. The β decay of ^{20}Na proceeds 20% of the time to α-unstable levels in ^{20}Ne and provides calibration lines in the region of the ^{8}B α-spectrum peak.

The experiment was performed using the ATLAS superconducting linear accelerator at the Argonne National Laboratory. A ^{8}B beam was produced with the in-flight technique [21] using the ^{3}He(^{6}Li, ^{8}B)n reaction. A 36.4 MeV ^{6}Li beam was incident on a 3.5 cm long gas cell filled with 700 mbar of ^{3}He and cooled to 82 K. The pressure and temperature in the cell were held constant to ±1%. The ^{8}B reaction products were separated from the primary ^{6}Li beam with a 22° bending magnet and transported into the focal plane of the Enge Split Pole spectrograph where they were identified with respect to mass, charge, and energy in the gas-filled focal plane detector [22]. The magnetic field in the spectrograph was then adjusted to implant 27.3 MeV ^{8}B ions into the 91 μm thick Si detector positioned in the focal plane adjacent to the gas-filled detector. Stopping simulations [23] give the range of the ^{8}B ions in the silicon to be 42.3 ± 2.0 μm. An 11 mm diameter Ta collimator in front of the Si detector ensured that the ^{8}B ions were implanted only into the central region of the detector.

A 25 mm diameter ×2 mm thick plastic scintillator, coupled by a light guide to a Hamamatsu R647 photomultiplier tube, was positioned 12 mm behind the Si detector. The plastic scintillator, operated in coincidence, selected events where the β-particle trajectory was within ~40° to the normal of the Si detector. This provided a sample of events with minimum energy deposition by the β particle. The Si/scintillator detector system was cooled to −5 °C. A schematic representation of the apparatus is shown in Fig. 2.

The ^{6}Li beam was cycled (1.5 s on/1.5 s off) and data taken only during the beam-off cycle. With an average ^{6}Li current of 60 pnA about three ^{8}B ions/s were implanted. Energy signals and the relative timing between the Si and β detectors were recorded, as well as the timing of the Si signal with respect to the beam-off cycle. Over three days, 4.5×10^5 ^{8}B events were observed, 16% of which were in coincidence with an event in the β detector.

The system was calibrated using a beam of the β-delayed α emitter ^{20}Na ($t_{1/2}$ = 448 ms) immediately before the ^{8}B run. The ^{20}Na beam was produced using the same in-flight technique with a 199 MeV ^{19}F beam via the ^{3}He(^{19}F, ^{20}Na)2n reaction. The spectrograph selected ^{20}Na ions of 170 MeV which passed through a Mylar slowing foil before being implanted into the Si detector.

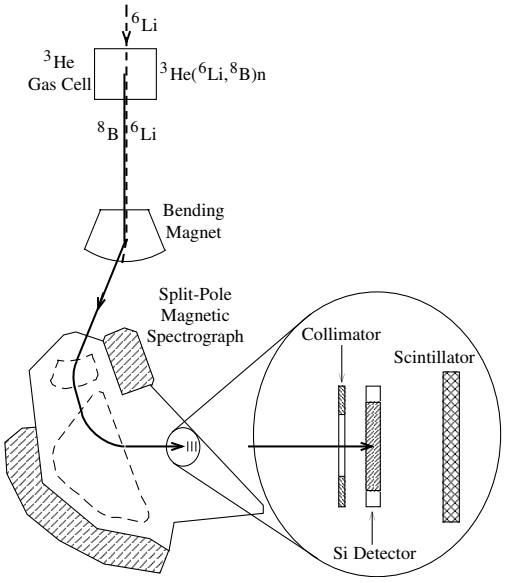

FIG. 2. The experimental setup used to produce ^{8}B(^{20}Na), separate it from the primary ^{6}Li(^{19}F) beam, and select ions with energy 27.3 MeV (170 MeV) for implantation into the Si detector (not to scale).

Stopping simulations [23] indicate the range of the ^{20}Na to be 48 ± 6 μm, which gives an uncertainty in the β-particle energy deposition of ± 3 keV for coincidence events. The three largest alpha-emitting branches in ^{20}Na decay, with alpha energy releases of 2691.9(1.2), 3099.0(2.2), and 5544.0(2.8) keV [24], provide calibration. Data acquisition was identical to the ^{8}B runs, but the on-off cycle time was reduced to 1 s on/1 s off. With a 0.5 pnA ^{19}F beam, about eight ^{20}Na decays/min were detected in the Si detector, resulting in 1.0×10^4 ^{20}Na events over a one day run. Spectra from the implanted ^{8}B and ^{20}Na are shown in Fig. 3.

The pulse height defect associated with the recoil ^{16}O nucleus, which carries one-fifth of the energy of the alpha disintegration in the ^{20}Na decay, has been measured for ^{16}O nuclei in the energy range of interest [25]. The correction is 40–50 keV for the various ^{20}Na alpha lines, with an uncertainty of ± 5 keV.

During the implantation process, the ion flux incident on the Si detector was monitored by the spectrograph focal plane detector. The ion flux, consisting primarily of ions from the low energy tails of the primary ^{19}F and ^{6}Li beams, was an order of magnitude below the threshold for detector damage [26], and no gain variation due to damage was expected. The gain was monitored by observing the centroid of the ^{8}B energy spectrum which was found to fluctuate within a range of $\pm 0.25\%$, which corresponds to ± 7 keV at the spectrum peak. These fluctuations in gain are not corrected for, but are included as, an uncertainty in the energy scale.

The β-detector coincidence requirement allowed rejection of events in the Si detector associated with ions accelerated by ATLAS during the beam-off cycle. The exception is protons, which did not stop in the Si detector and triggered a coincidence count in the β detector. These produced a peak near 800 keV in the coincidence data. As a result, the data below 1.2 MeV were not used in the analysis. Extrapolation of the data to excitation energies below 1.2 MeV, which account for 10^{-3} of all decays, was performed using the R-matrix approach. Uncertainties in the extrapolation were estimated by varying the Coulomb matching radius between 4.0 and 5.0 fm.

Detector resolution consisted of a noise component, a β-particle energy loss component, and a contribution from the recoil of the daughter nucleus following the β decay. The noise width was estimated using electronic pulsers. The effect of β-particle energy loss, which was modeled using EGSnrc software [27], lowered the peak of the coincidence data by 24 keV, as compared to 55 keV for the total data. After the correction, the peaks of the coincidence and total spectra agree within 2 keV, which we adopt as an estimate of uncertainty in the EGSnrc simulation. The ^{8}Be nuclear recoil following β decay is exactly calculable and contributes 7 keV at the α-spectrum peak.

The ^{8}Be excitation energy profile following ^{8}B β decay was determined by correcting the data for detector resolution, and extending to energies below 1.2 MeV. The dominant uncertainty is the ambiguity in energy scale induced by the gain variation. The uncertainties from calibration, implantation depth, β-particle energy deposition, and extrapolation to low energies have also been considered. Overall, the uncertainty in the energy scale at the spectrum peak is ± 9 keV. The numerical results are available in [28].

The measurement reported here disagrees with the result of Ortiz *et al.* [12]. For both measurements, the inferred neutrino spectrum is far more dependent on the systematic uncertainties in the α spectrum than on the statistical uncertainties. Smooth R-matrix fits to the data thus provide a convenient method of comparing the two results. Figure 4 shows a comparison of the present results and a fit to the data of Ortiz *et al.*, reported in [29]. Uncertainties in the Ortiz *et al.* curve are taken directly from [29].

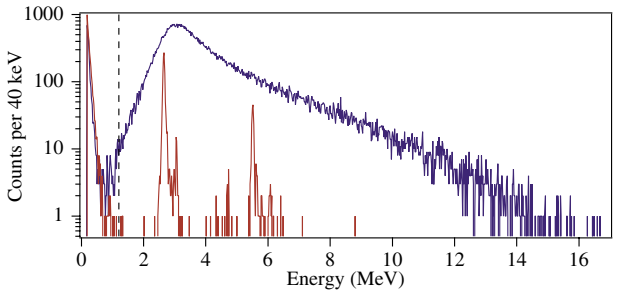

FIG. 3 (color). The measured ^{8}B β-delayed alpha spectrum (blue) shown with the β-delayed alpha lines from the ^{20}Na calibration source (red). The data shown here correspond to events coincident with the beta detector. Only ^{8}B events above 1.2 MeV (dashed line) are used in the analysis.

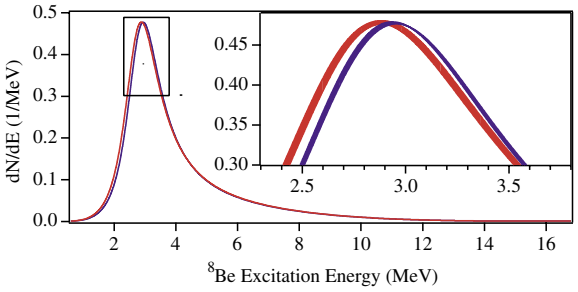

FIG. 4 (color). R-matrix fits to the ^{8}Be energy profile determined in this work (blue) and in Ortiz *et al.* (red). The spectra have been normalized to share the same peak height. The inset shows the locations of the spectrum peaks, on which the neutrino spectrum is highly dependent. The width of the lines in the inset indicates the magnitude of the $\pm 1\sigma$ experimental uncertainties. The thin feature in the blue curve arises because the dominant uncertainty is a multiplicative factor in the energy scale.

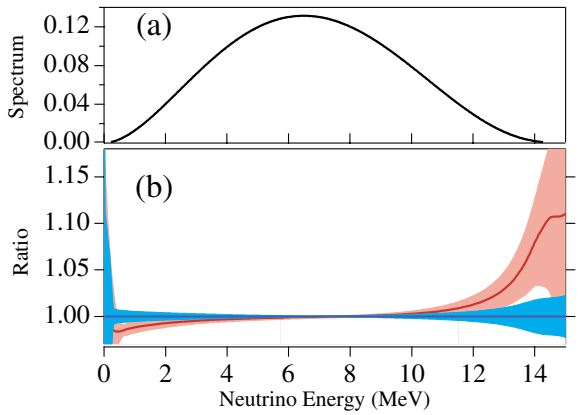

FIG. 5 (color). (a) The normalized neutrino energy spectrum deduced from this measurement. (b) The red line is the ratio between the neutrino spectrum recommended by Ortiz *et al.* [29] to the spectrum deduced in this work. The blue line represents the spectrum deduced here. The bands indicate the $\pm 1\sigma$ experimental uncertainties, which are the result of propagating the uncertainties in the alpha spectrum, shown in Fig. 4, to the neutrino spectrum. The Ortiz *et al.* spectrum was smoothed to account for binning effects.

The ^{8}B β spectrum was deduced from the α spectrum measured here. Radiative corrections [30] and recoil order effects [19] were applied. These corrections contribute to the spectrum at the 5% level. This deduced β spectrum was compared to the experimental spectrum [18], and gave an agreement of $\chi^2/\mathrm{dof} = 32.9/31$, where only statistical uncertainties were included in the minimization function. The β spectrum deduced by Ortiz must be shifted by an energy offset of -70 ± 20 keV to give agreement ($\chi^2/\mathrm{dof} = 31.8/31$) with the data [12]. When the β spectrum deduced here was similarly allowed to float by an energy offset, best agreement ($\chi^2/\mathrm{dof} = 32.5/31$) was found for an offset of -13 ± 20 keV. The calibration uncertainty of the β-spectrum measurement is reported as 25 keV [17].

The ^{8}B neutrino spectrum was deduced from our data, with recoil order corrections identical to those for the β spectrum, and radiative corrections from [31]. The neutrino spectrum is available in numerical form in [28]. Comparison of the ^{8}B neutrino spectrum recommended by Ortiz *et al.* [29] to the spectrum determined here is shown in Fig. 5. It must be emphasized that the disagreement between the α-spectrum measurement reported here and the measurement of Ortiz *et al.* is more serious than is indicated in Fig. 5. We are unable to reproduce the neutrino spectrum of Ortiz *et al.* based on their reported α spectrum, both of which are listed in tabular form in [29]. The disagreement between the neutrino spectrum based on our measurement and the spectrum we obtain from the Ortiz *et al.* α-spectrum data is roughly 50% larger than the disagreement indicated in Fig. 5 for neutrinos above 12 MeV.

The inconsistencies in the deduced ^{8}B neutrino spectra, shown in Fig. 5, are comparable to the precision with which Super-Kamiokande has measured the differential energy spectrum of solar neutrinos [20]. Interpretation of solar neutrino shape measurements will become increasingly dependent on the uncertainties in the ^{8}B α spectrum as neutrino data become more precise.

This work was supported by the Department of Energy under Contracts No. W-31-109-ENG-38 and No. DE-AC03-76SF00098.

[1] R. Davis, Jr., D. S. Harmer, and K. C. Hoffman, Phys. Rev. Lett. **20**, 1205 (1968).
[2] J. N. Bahcall, N A. Bahcall, and G. Shaviv, Phys. Rev. Lett. **20**, 1209 (1968).
[3] J. N. Bahcall, M. C. Gonzalez-Garcia, and C. Peña-Garay, J. High Energy Phys. **7**, 54 (2002), offers a review of the results and contains references to the experiments.
[4] J. N. Bahcall *et al.*, Astrophys. J. **555**, 990 (2001).
[5] Q. R. Ahmad *et al.*, Phys. Rev. Lett. **89**, 011301 (2002).
[6] K. Eguchi *et al.*, Phys. Rev. Lett. **90**, 021802 (2003).
[7] N. Heydenburg and G. Temmer, Phys. Rev. **104**, 123 (1956).
[8] T. Tombrello and L. Senhouse, Phys. Rev. **129**, 2252 (1963).
[9] B. J. Farmer and C. M. Class,Nucl. Phys. **15**, 626 (1960).
[10] L. De Braeckeleer *et al.*, Phys. Rev. C **51**, 2778 (1995).
[11] D. H. Wilkinson and D. E. Alburger, Phys. Rev. Lett. **26**, 1127 (1971).
[12] C. E. Ortiz, A. Garcia, R. A. Waltz, M. Bhattacharya, and A. K. Komives, Phys. Rev. Lett. **85**, 2909 (2000).
[13] F. C. Barker, Aust. J. Phys. **22**, 293 (1969).
[14] E. K. Warburton, Phys. Rev. C **33**, 303 (1986).
[15] F. C. Barker, Aust. J. Phys. **42**, 25 (1989).
[16] M. Bhattacharya and E. G. Adelberger, Phys. Rev. C **65**, 055502 (2002).
[17] J. N. Bahcall *et al.*, Phys. Rev. C **54**, 411 (1996).
[18] J. Napolitano *et al.*, Phys. Rev. C **36**, 298 (1987).
[19] J. N. Bahcall and B. R. Holstein, Phys. Rev. C **33**, 2121 (1986).
[20] S. Fukuda *et al.*, Phys. Rev. Lett. **86**, 5651 (2001).
[21] B. Harss *et al.*, Rev. Sci. Instrum. **71**, 380 (2000).
[22] K. E. Rehm and F. L. H. Wolfs, Nucl. Instrum. Methods Phys. Res., Sect. A **273**, 262 (1988).
[23] J. F. Ziegler, http://www.srim.org.
[24] F. Ajzenberg-Selove, Nucl. Phys. **A490**, 1 (1988).
[25] W. N. Lennard *et al.*, Nucl. Instrum. Methods Phys. Res., Sect. A **248**, 454 (1986).
[26] Introduction to Charged Particle Detectors (Ortec, 2003), http://www.ortec-online.com/detectors/chargedparticle/introduction/radiation.htm.
[27] http://www.sao.nrc.ca/inms/irs/EGSnrc/EGSnrc.html.
[28] W. T. Winter *et al.*, Phys. Rev. Cto be published).
[29] http://www.nd.edu/~nsl/BeyondSM/boron8/tables.
[30] A. Sirlin, Phys. Rev. **164**, 1767 (1967).
[31] I. S. Batkin and M. K. Sundaresan, Phys. Rev. D **52**, 5362 (1995).